A comparison of two control laws for semi-active suspensions

A comparison of two control laws for semi-active suspensions

Maurice Rienks

WFW Report 94.036

Eindhoven, March 1994

Coaches: Ir. J.H.E.A Muijderman
Dr.Ir. F.E. Veldpaus

Eindhoven University of Technology
Faculty of Mechanical Engineering
Systems and Control Group

Abstract

A quarter-vehicle model is used to compare two control strategies for a semi-active suspension at the rear side of the tractor of a tractor-semitrailer combination. One strategy is based on the Clipped Optimal Method and the other strategy is based on the Steepest Gradient Method. Simulations have been excecuted for different roads and different vehicle parameters. It is shown that the performance of the strategies depends on this set of vehicle parameters.

Contents

Chapter 1

Introduction

The ride quality of a vehicle can be improved by the application of an active suspension. An active suspension can reduce the chassis accelerations, the suspension deflection and the dynamic tire load. This results in a better comfort of the vehicle, and a reduction in road damage. This improvement of the dynamic behaviour is attained by putting energy into and out of the system via an actuator.
An active suspension has the following two major drawbacks:
- The actuators in active suspensions require large power,
- The malfunction of controllers may cause catastrophic failure of the vehicle.

An alternative is the application of a semi-active suspension. Semi-active suspensions are conventional suspensions with additional controllable shockabsorbers. No energy is put into the system. Semi-active suspensions only require a power source to change the damper rate of the shockabsorbers.
To control the suspension a number of strategies has been developed. In this report two control laws, namely the Clipped Optimal Control Law [2] and the Steepest Gradient Control Law [1] will be compared. The comparison will be based mainly on simulation results.

Chapter 2

Formulation of the problem

2.1 Vehicle model

To simulate the dynamic behavior of a vehicle with semi-active suspension a quarter vehicle model is used. This model is shown in Fig. 1.1.

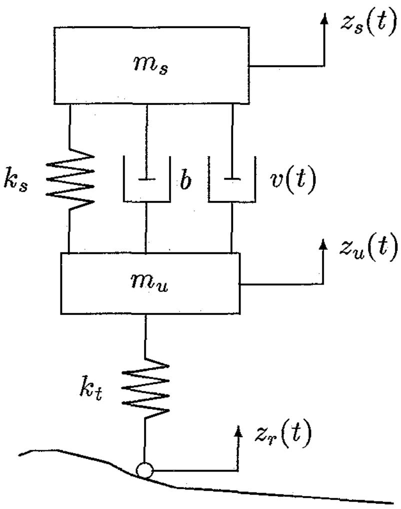

m_s	[kg]	chassis mass
m_u	[kg]	unsprung mass
k_s	[N/m]	suspension stiffness
k_u	[N/m]	tire stiffness
b	[Ns/m]	constant dampingcoefficient
v	[Ns/m]	variable dampingcoefficient

Fig 1.1: Vehicle model

The corresponding mathematical model can be expressed in state space form by the following differential equation:

$$\dot{x} = A_0 x + \Phi(x) v + L \dot{z}_r \tag{2.1}$$

where:

- x is the statespace vector defined as:

$$x = \begin{bmatrix} x_1 \\ x_2 \\ x_3 \\ x_4 \end{bmatrix} = \begin{bmatrix} z_s - z_u \\ \dot{z}_s \\ z_u - z_r \\ \dot{z}_u \end{bmatrix} = \begin{bmatrix} \text{suspension deflection} \\ \text{sprung mass velocity} \\ \text{tire deflection} \\ \text{unsprung mass velocity} \end{bmatrix}$$

- v, the variable dampingcoefficient of the shockabsorber, is the system input. The values of v are limited by $0 \leq v \leq v_{max}$.

- $\dot{z}_r$, the road velocity, is considered as a disturbance of the system.

- The system-, input- and the disturbancematrix are respectively:

$$
\begin{aligned}
A_0 &= \begin{bmatrix} 0 & 1 & 0 & -1 \\ -\frac{k_s}{m_s} & -\frac{b}{m_s} & 0 & \frac{b}{m_s} \\ 0 & 0 & 0 & 1 \\ \frac{k_s}{m_u} & \frac{b}{m_u} & -\frac{k_t}{m_u} & -\frac{b}{m_u} \end{bmatrix} \\
\Phi(x) &= -B(x_2 - x_4) \; ; \; B = \begin{bmatrix} 0 & \frac{1}{m_s} & 0 & -\frac{1}{m_u} \end{bmatrix}^T \\
L &= \begin{bmatrix} 0 & 0 & -1 & 0 \end{bmatrix}^T
\end{aligned}
$$

The passive system is defined as the system without systeminput, i.e. $v = 0$. The passive system is stable if $b > 0$.

2.2 Road model

The control laws will be derived for the transient response case, i.e. assuming no road velocity disturbance, $\dot{z}_r(t) = 0$, and an initial condition disturbance unequal to zero, $x(0) \neq 0$. The reason for this assumption is that it simplifies derivation of the control laws substantial. Later, during the simulations it is tested how both stratagies behave on other roads.

2.3 Design Objective

The objective of the semi-active suspension is to minimize the chassis acceleration under the conditions that the suspension working space is not exceeded and that the tire does not loose contact with the road, i.e.

$$-0.09 \leq z_s - z_u \leq 0.14\,[m] \tag{2.2}$$

$$z_u - z_r \leq 0.015\,[m] \tag{2.3}$$

In order to be able to derive both control laws this objective is translated into the minimization of a performance index, which is a quadratic function of the chassis acceleration, the suspension space and the tire deflection, i.e.

$$J = \lim_{T \to \infty} \int_0^T [\ddot{z}_s^2 + q_1(z_s - z_u)^2 + q_2(z_u - z_r)^2]dt \tag{2.4}$$

where q_1 and q_2 are weighting factors. q_1 and q_2 have to be chosen such that the body acceleration is minimal and that the conditions (2.2) and (2.3) are satisfied. In practice it appears to be difficult to satisfy these conditions.

The performance index J, (2.4) can be rewritten as:

$$J = \lim_{T\to\infty} \int_0^T (x^T Q_1 x + \dot{x}^T Q_a \dot{x})dt \tag{2.5}$$

where $Q_1 > 0$, $Q_a \geq 0$:

$$Q_1 = \begin{bmatrix} q_1 & 0 & 0 & 0 \\ 0 & 0 & 0 & 0 \\ 0 & 0 & q_2 & 0 \\ 0 & 0 & 0 & 0 \end{bmatrix} ; \; Q_a = \begin{bmatrix} 0 & 0 & 0 & 0 \\ 0 & 1 & 0 & 0 \\ 0 & 0 & 0 & 0 \\ 0 & 0 & 0 & 0 \end{bmatrix}$$

When the equation of motion without the road velocity disturbance, is substituted into (2.5), the performance index becomes:

$$J = \lim_{T\to\infty} \int_0^T [x^T (Q_1 + A_0^T Q_a A_0)x + vx^T (N^T Q_a A_0 + A_0^T Q_a N)x + vx^T N^T Q_a N x v]dt \tag{2.6}$$

Or,

$$J = \lim_{T\to\infty} \int_0^T [x^T Q_0 x + 2vS(x)x + vR(x)v]dt \tag{2.7}$$

where, Q_0 is derived from a passive term while $R(x)$ and $S(x)$ are derived from a semi-active term:

$$\begin{aligned} Q_0 &= Q_1 + A_0^T Q_a A_0 \\ R(x) &= R_0 (x_2 - x_4)^2 \; ; \; R_0 = \frac{1}{{m_s}^2} \\ S(x) &= -S_0 (x_2 - x_4) \; ; \; S_0 = \begin{bmatrix} \frac{-k_s}{{m_s}^2} & \frac{-b}{{m_s}^2} & 0 & \frac{b}{{m_s}^2} \end{bmatrix} \end{aligned}$$

2.4 Problem description

Now the problem can be formulated as follows: find the dampingcoefficient that minimizes the performance index J subject to the differential equation constraint, the saturation bound and the initial condition:

$$\text{minimize} \quad J = \lim_{T\to\infty} \int_0^T F dt \text{ where, } F = [x^T Q_0 x + 2vS(x)x + vR(x)v]dt$$

$$\text{while:} \quad \dot{x} = A_0 x + \Phi(x) v \tag{2.8}$$

$$0 \leq v \leq v_{max} \tag{2.9}$$

$$x\ (0) = x_0 \tag{2.10}$$

Chapter 3

Derivation of the Clipped Optimal Control Law (COC)

In this chapter the Clipped Optimal Control Law (COC) will be derived by adding the constraint equations (2.8) and (2.9) to the performance index by means of the Lagrange multiplier method. By applying the calculus of variations this extended performance index will be minimized. This yields the control law for the damping coefficient v.

With the Lagrange multiplier method the problem of making J stationary under abovementioned constraints can be replaced by the problem of making $\bar{J}$ stationary without constraints. $\bar{F}$ becomes:

$$\bar{F} = x^T Q_0 x + 2v^T S(x)x + v^T R(x)v + 2p^T(A_0 x + \Phi(x)v - \dot{x}) - 2\lambda_1 v + 2\lambda_2(v - v_{max}) \quad (3.1)$$

where p is a Lagrange multiplier vector for the differential equation constraint (2.8) and $\lambda_1 \geq 0$ and $\lambda_2 \geq 0$ are Lagrange multipliers for the satutation boundary constraint (2.9). When the lower constraint of v is active $\lambda_1 > 0$ and $\lambda_2 = 0$, when the upper constraint is active $\lambda_2 > 0$ and $\lambda_1 = 0$. No saturation implies that both λ_1 and λ_2 are zero.

We wish to find the function v that makes $\bar{J}$ stationary. This means, find the function v such that

$$\delta\bar{J}(v, p, x, \dot{x}, \lambda_1, \lambda_2) = 0 \quad (3.2)$$

By means of the calculus of variations $\delta\bar{J}$ can be written as follows:

$$\delta\bar{J} = \lim_{T\to\infty} \int_0^T \{\frac{\partial\bar{F}}{\partial v}\delta v + \frac{\partial\bar{F}}{\partial p}\delta p + \frac{\partial\bar{F}}{\partial x}\delta x + \frac{\partial\bar{F}}{\partial\dot{x}}\delta\dot{x} + \frac{\partial\bar{F}}{\partial\lambda_1}\delta\lambda_1 + \frac{\partial\bar{F}}{\partial\lambda_2}\delta\lambda_2\}dt \quad (3.3)$$

Partial integration of the fourth term on the right hand side yields:

$$\lim_{T\to\infty} \int_0^T \{\frac{\partial\bar{F}}{\partial\dot{x}}\delta\dot{x}\}dt = \lim_{T\to\infty} \int_0^T \{-\frac{d}{dt}\left[\frac{\partial\bar{F}}{\partial\dot{x}}\right]\delta x\}dt + \lim_{T\to\infty}\left[\frac{\partial\bar{F}}{\partial\dot{x}}\delta x\right]_0^T \quad (3.4)$$

Now $\delta\bar{J}$ becomes

$$\delta\bar{J} = \lim_{T\to\infty}\int_0^T\{\frac{\partial\bar{F}}{\partial v}\delta v + \frac{\partial\bar{F}}{\partial p}\delta p + \left(\frac{\partial\bar{F}}{\partial x} - \frac{d}{dt}\left[\frac{\partial\bar{F}}{\partial\dot{x}}\right]\right)\delta x + \qquad (3.5)$$

$$+ \frac{\partial\bar{F}}{\partial\lambda_1}\delta\lambda_1 + \frac{\partial\bar{F}}{\partial\lambda_2}\delta\lambda_2\}dt + \lim_{T\to\infty}\left[\frac{\partial\bar{F}}{\partial\dot{x}}\delta x\right]_0^T \qquad (3.6)$$

Since $\delta\bar{J}$ must be zero, the following equations are found:

1. $\frac{\partial\bar{F}}{\partial v} = 0$

$$\Longrightarrow v = -R^{-1}(x)\Phi^T(x)p - R^{-1}(x)S(x)x + R^{-1}(x)(\lambda_1 - \lambda 2) \qquad (3.7)$$

   Note that v is undefined if $R(x) \to 0$. If $R(x) \to 0$, i.e. the relative velocity of the chassis mass and the sprung mass tends to zero, the damper force also tends to zero so the value of v is not of any interest. This is the reason why v can be chosen arbitrarly within the saturation bound.

2. $\frac{\partial\bar{F}}{\partial p} = 0$

$$\overset{(3.7)}{\Longrightarrow} \dot{x} = (A_0 - BR_0^{-1}S_0)x - BR_0^{-1}B^Tp + \Phi(x)R^{-1}(x)(\lambda_1 - \lambda_2) \qquad (3.8)$$

3. $\frac{\partial\bar{F}}{\partial x} - \frac{d}{dt}\left[\frac{\partial\bar{F}}{\partial\dot{x}}\right] = 0$

$$\overset{(3.7)}{\Longrightarrow} -\dot{p} = [Q_0 - S_0^TR_0^{-1}S_0]x + [A_0 - (BR_0^{-1}S_0)]^Tp + $$

$$+ [S^T(x)R^{-1}(x) + v^T(x_2 - x_4)^{-1}\begin{bmatrix}0\\1\\0\\-1\end{bmatrix}](\lambda_1 - \lambda_2) \qquad (3.9)$$

4. $\lim_{T\to\infty}\left[\frac{\partial\bar{F}}{\partial\dot{x}}\delta x\right]_0^T = 0 \ \wedge\ \delta x(0) = 0$

$$\Longrightarrow \lim_{T\to\infty} p(T) = 0 \qquad (3.10)$$

5. $\frac{\partial\bar{F}}{\partial\lambda_1}\delta\lambda_1 + \frac{\partial\bar{F}}{\partial\lambda_2}\delta\lambda_2 = 0$

$$\Longrightarrow \begin{cases} \text{Case 1: } \frac{\partial\bar{F}}{\partial\lambda_1} = 0 \wedge \lambda_2 = 0 \Longrightarrow v = 0 \\ \text{Case 2: } \lambda_1 = 0 \wedge \lambda_2 = 0 \overset{(3.7)}{\Longrightarrow} v = -R^{-1}(x)\Phi^T(x)p - R^{-1}(x)S(x)x \\ \text{Case 3: } \frac{\partial\bar{F}}{\partial\lambda_2} = 0 \wedge \lambda_1 = 0 \Longrightarrow v = v_{max} \end{cases} \qquad (3.11)$$

By taking equation (3.7) into consideration the Lagrange multipliers and their condition, can be obtained as follows.

$$\begin{array}{lll} \text{Case 1:} & \lambda_1 = (\Phi^T(x)p + S(x)x), \lambda_2 = 0 & \text{if } (\Phi^T(x)p + S(x)x) > 0 \\ \text{Case 2:} & \lambda_1 = 0, \lambda_2 = 0 & \text{if } -R(x)v_{max} \leq (\Phi^T(x)p + S(x)x) \leq 0 \\ \text{Case 3:} & \lambda_1 = 0, \lambda_2 = -(\Phi^T(x)p + S(x)x) - R(x)v_{max} & \\ & & \text{if } (\Phi^T(x)p + S(x)x) < -R(x)v_{max} \end{array} \quad (3.12)$$

After substitution of (3.12) into (3.8) and (3.9) it can be concluded that we have found an expression for $v(x,p)$, (3.11), two coupled linear differential equations in x and p, resp. (3.8) and (3.9), and their conditions (2.10) and (3.10). To obtain p and x for the three cases these differential equations have to be solved. This problem can be written as follows:

$$\begin{bmatrix} \dot{x} \\ \dot{p} \end{bmatrix} = \begin{bmatrix} A & R \\ -Q & -A^T \end{bmatrix} \begin{bmatrix} x \\ p \end{bmatrix} ; \begin{bmatrix} x(0) \\ \lim_{T\to\infty} p(T) \end{bmatrix} = \begin{bmatrix} x_0 \\ 0 \end{bmatrix} \quad (3.13)$$

where,

	Case 1.	Case 2.	Case 3.
	$v = 0$	$0 < v < v_{max}$	$v = v_{max}$
A	A_0	$A_0 - BR_0^{-1}S_0$	$A_0 + Nv_{max}$
R	0	$-BR_0^{-1}B^T$	0
Q	Q_0	$Q_0 - S_0^T R_0^{-1} S_0$	$Q_0 + Q_{v]v=v_{max}}$

To solve Eq. (3.13) it is assumed that $p(t)$ can be written as:

$$p(t) = P(t)x(t) \quad (3.14)$$

By substitution of Eq. (3.14) into Eq. (3.13) the problem of solving x and p can be translated into solving P from the following Matrix Riccati Equation (MRE):

$$\begin{cases} -\dot{P}(t) = P(t)A + A^T P(t) + P(t)RP(t) + Q \\ \lim_{T\to\infty} P(T) = 0 \end{cases} \quad (3.15)$$

To obtain the optimal v, we have to solve the system equation (2.8) under initial condition (3.8) and the time varying, state dependent Ricatti equation (3.15). Since this set of differential equations is not linear and no analytical solution can be obtained, we can not express the optimal control as an explicit function of x.
To get a practical control law, the matrix $P(t)$ is replaced by a contant matrix P solved from the unconstrained case (Case 2.), i.e. from the following Algebraic Riccati Equation (ARE):

$$0 = P(A_0 - BR_0^{-1}S_0) + (A_0 - BR_0^{-1}S_0)^T P - PBR_0^{-1}B^T P + (Q_0 - S_0^T R_0^{-1} S_0) \quad (3.16)$$

where we have assumed no saturation and assigned $\dot{P} = 0$ as T goes to infinity. This assumption that implies that the MRE can be simplified to an ARE is in fact not correct because of the switches of the matrices A, R and Q for the three different cases.

Finally, the sub-optimal Clipped Optimal Control Law can be written as follows:

$$v = \begin{cases} 0 & \text{if } (\Phi^T(x)P + S(x))x > 0 \\ -R^{-1}(x)(\Phi^T(x)P + S(x))x & \text{if } -R(x)v_{max} \leq (\Phi^T(x)P + S(x))x \leq 0 \\ v_{max} & \text{if } (\Phi^T(x)P + S(x))x < -R(x)v_{max} \end{cases} \quad (3.17)$$

This result has been obtained by making $\tilde{F}$ stationary which does not automatically mean that $\tilde{F}$ is minimum. It can be proved that for this case $\tilde{F}$ is minimum.

Chapter 4

Derivation of the Steepest Gradient Control Law (SGC)

The performance index, which has to be minimized, can be divided in the performance index for the passive system, $J_{passive}$ and an additional term. The additional term contains the contribution of the semi-active damper. The following derivation shows that the Steepest Gradient Control Law (SGC) minimizes the integrand of this additional term. This finally leads to an expression for the damping coefficient v.

First we derive a relation for the performance index of the passive system, $J_{passive}$. This is the performance index in case of no systeminput, $v = 0$. When $v = 0$ is substituted into (2.7) the relation for $J_{passive}$ follows:

$$J_{passive} = \lim_{T\to\infty} \int_0^T x_p^T Q_0 x_p dt \tag{4.1}$$

where x_p the state vector of the passive system. At the same time $J_{passive}$ can be written as:

$$J_{passive} = V(x_p(0)) \qquad \text{where} \qquad V(x_p(t)) = x_p(t)^T P x_p(t) \tag{4.2}$$

By taking Eq. (4.1) and Eq. (4.2) into consideration and assuming some passive damping for stability, an expression for P can be derived as follows:

$$\lim_{T\to\infty} \int_0^T x_p^T Q_0 x_p dt = V(x_p(0)) \tag{4.3}$$

$$= \lim_{T\to\infty} \int_0^T -\dot{V}(x_p) dt^{\dagger} \tag{4.4}$$

$$= \lim_{T\to\infty} \int_0^T -(\dot{x}_p^T P x_p + x_p^T P \dot{x}_p) dt \tag{4.5}$$

Using the equation of motion of the passive system, $\dot{x}_p = A_0 x_p$, $\dot{x}_p$ can be eliminated:

$$\lim_{T\to\infty} \int_0^T x_p^T Q_0 x_p dt = \lim_{T\to\infty} \int_0^T -x_p^T (A_0^T P + P A_0) x_p dt \tag{4.6}$$

This results in the following relation for P:

$$A_0^T P + P A_0 = -Q_0 \tag{4.7}$$

† Since $\lim_{T\to\infty} \int_0^T -\dot{V}(x_p)dt = \lim_{T\to\infty} -V(x_p(T)) + V(x_p(0)) = V(x_p(0))$

So the expression of $J_{passive}$ can be written as:

$$J_{passive} = V(x_p(0)) = x_p^T(0)Px_p(0) \quad \text{with: } A_0^TP + PA_0 = -Q_0 \tag{4.8}$$

Now we will look at the semi-active suspension. We want to write the performance index of the semi-active system as the sum of $J_{passive}$ and an additional term.
First we consider $\dot{V}(x)$ for the semi-active system, where x is the state space vector of the semi-active system. When Eq. (4.2) is differentiated with respect to t and $\dot{x}$ is eliminated by using the equation of motion of the semi-active system Eq. (2.8), $\dot{V}$ becomes:

$$\dot{V}(x) = x^T(PA_0 + A_0^TP)x + 2v\Phi^T(x)Px \tag{4.9}$$

When expression (4.7) is substituted into (4.9) the following expression for $\dot{V}(x)$ follows:

$$\dot{V}(x) = -x^TQ_0x + 2v\Phi^T(x)Px \tag{4.10}$$

According to (2.7) the performance index of the semi-active system is:

$$J = \lim_{T\to\infty}\int_0^T [x^TQ_0x + 2v^TS(x)x + v^TR(x)v]dt$$

When the first term of the right side of equation (4.10) is substituted into this performance index, J becomes:

$$J = \lim_{T\to\infty}\int_0^T [-\dot{V}(x) + 2v^T(\Phi^T(x)P + S(x))x + v^TR(x)v]dt \tag{4.11}$$

Since the system is assumted to be stable J becomes:

$$J = V(x(0)) + \lim_{T\to\infty}\int_0^T [2v^T(\Phi^T(x)P + S(x))x + v^TR(x)v]dt \tag{4.12}$$

By means of equation (4.2) and the knowledge that $x(0) = x_p(0)$, the performance index of the semi-active system can be written as:

$$\begin{aligned} J &= J_{passive} + \lim_{T\to\infty}\int_0^T [2v^T(\Phi^T(x)P + S(x))x + v^TR(x)v]dt \\ &= J_{passive} + \lim_{T\to\infty}\int_0^T \tilde{F}(v, x(t))dt \end{aligned} \tag{4.13}$$

Now, a semi-active control law is proposed that stationizes the value of $\tilde{F}(v)$, so

$$\frac{\partial \tilde{F}}{\partial v} = 0 \;\Rightarrow\; v = -R(x)^{-1}(\Phi^T(x)P + S(x))x \tag{4.14}$$

Since $\frac{\partial^2 \tilde{F}}{\partial v^2} > 0 \;\forall\; R(x) \neq 0$[‡] it can be concluded that $\tilde{F}(v)$ is minimized.

When the saturation bound constraint (2.9) is taken into account the Steepest Gradient control v can be written as follows:

$$v = \begin{cases} 0 & \text{if } (\Phi^T(x)P + S(x))x \geq 0 \\ -R(x)^{-1}(\Phi^T(x)P + S(x))x & \text{if } -R(x)v_{max} < (\Phi^T(x)P + S(x))x < 0 \\ v_{max} & \text{if } (\Phi^T(x)P + S(x))x < -R(x)v_{max} \end{cases} \tag{4.15}$$

[‡] If $R(x) = 0$ then the value of v is not of any interest

By substitution of (4.15) into (4.13) it can be shown that $\tilde{F}$ is less than or equal to zero for all $t > 0$. So it can be concluded that the Steepest Gradient controlled system equals or improves the performance of the passive system.

The results of Chapter 3 and Chapter 4 show that the Clipped Optimal Control Law and the Steepest Gradient Control Law share the same structure. The only difference is the procedure to determine P: P_{coc} is solved from the Algebraic Riccati Equation and P_{sgc} from the Lyapunov Equation.

Chapter 5

A Comparison of COC and SGC

5.1 Prelude

To investigate the difference in the dynamic behaviour of the Clipped Optimal controlled and the Steepest Gradient controlled vehicle various simulations were performed by using the quarter-vehicle model.
Simulations have been executed for different excitations. These excitations are initial disturbances, rounded pulses and a stochastic road.
At the same time simulations have been performed for different vehicle parameters. Saturation bounds as well as weighting factors are varied.
The used numerical values of the vehicle parameters for the $\frac{1}{4}$-car model are:

chassis mass	m_s	8650	[kg]
unsprung mass	m_u	1350	[kg]
suspension stiffness	k_s	4.4E5	[N/m]
tire stiffness	k_t	6.5E6	[N/m]

Unless mentioned otherwise, the numerical values of the following parameters are:

constant dampingcoefficient	b	2E4	[Ns/m]
variable dampingcoefficient	v_{max}	2.31E4	[Ns/m]
weighting factor of suspension space	q_1	1.5E3	[-]
weighting factor of tire deflection	q_2	8E3	[-]

5.2 Simulations with initial condition disturbances

Initial condition disturbances have been used for simulation because the two control laws are derived for this deterministic case. So eventhough it is not the most realistic excitation of the system, it is a good test to see how the control laws succeed in satisfying their design objective. Since the design objective is to minimize the performance index, the performance is used to judge the response of the system.

The Effect of Initial Conditions:

The performance index,

$$J = \lim_{T\to\infty} \int_0^T [\ddot{z}_s^2 + q_1(z_s - z_u)^2 + q_2(z_u - z_r)^2]dt \tag{5.1}$$

can be divided into three parts:

$$J_{acc} = \lim_{T\to\infty} \int_0^T \ddot{z}_s^2 dt \; ; \; J_{sus} = \lim_{T\to\infty} \int_0^T q_1(z_s - z_u)^2 dt \; ; \; J_{tire} = \lim_{T\to\infty} \int_0^T q_2(z_u - z_r)^2 dt \quad (5.2)$$

To investigate the differences between COC and SGC for the acceleration, the suspension- and the tire deflection, the following quantity is defined:

$$H = \left(\frac{J_{coc} - J_{sgc}}{J_{coc}}\right) 100\%$$

Tabel 5.2 shows H_{acc}, H_{sus}, H_{tire} and H for different initial conditions.

% Improvement of SGC relative to COC

Initial Condition x_o [(m) (m/s) (m) (m/s)]^T	H_{acc} (%)	H_{sus} (%)	H_{tire} (%)	H (%)
[-0.01 -0.24 0.008 -0.42]^T	-4.01	12.65	7.71	8.5E-1
[0.14 0 0.015 0]^T	-0.21	0.27	-0.17	-1.72E-3
[0 0 0.0394 0]^T	-2.37	4.66	10.86	3.2E-1
[0.1514 0 0 0]^T	-0.22	0.25	-0.17	-1.80E-3
[0.100 0 0 0]^T	-0.22	0.25	-0.17	-1.80E-3

Tabel 5.2 Comparison of Performance Index

The conclusion of this table is that both the Steepest Gradient Control law and the Clipped Optimal Control law perform differently for different initial condition disturbances. Due to the nonlinearity of the system no obvious trend can be found neither for H_{acc}, H_{sus} and H_{tire} nor for H.
Nevertheless, one relation can be recognized. The tabel shows that the initial condition /performance index ratio is independent of the amplitude of the initial condition. This independency has been proved by Butsuen and Hedrick [2] in 1989.

The Effect of Saturation Bounds:

From Chapter 3 we know that the Clipped Optimal Control law is optimal when no saturation occurs along the trajectory. So it can be expected that the performance of Clipped Optimal will improve when the saturation bound (v_{max}) increases.

To investigate the effect of saturation bounds we consider the proportional improvement of SGC relative to COC:

$$H = \left(\frac{J_{coc} - J_{sgc}}{J_{coc}}\right) 100\%$$

In figure 5.1 this quantity has been plotted versus v_{max} for different values of the constant dampingcoefficient b.
This figure illustrates that COC performs substantially better than SGC as v_{max} increases. And when b increases the improvement of COC decreases because than the optimal dampingcoefficient is smaller than b, so v will mainly be zero. When v equals zero no difference exist in the performance of COC and SGC.
In the case of severe saturation SGC performs a few percents better than COC.
These conclusions hold good for different initial condition disturbances and for different

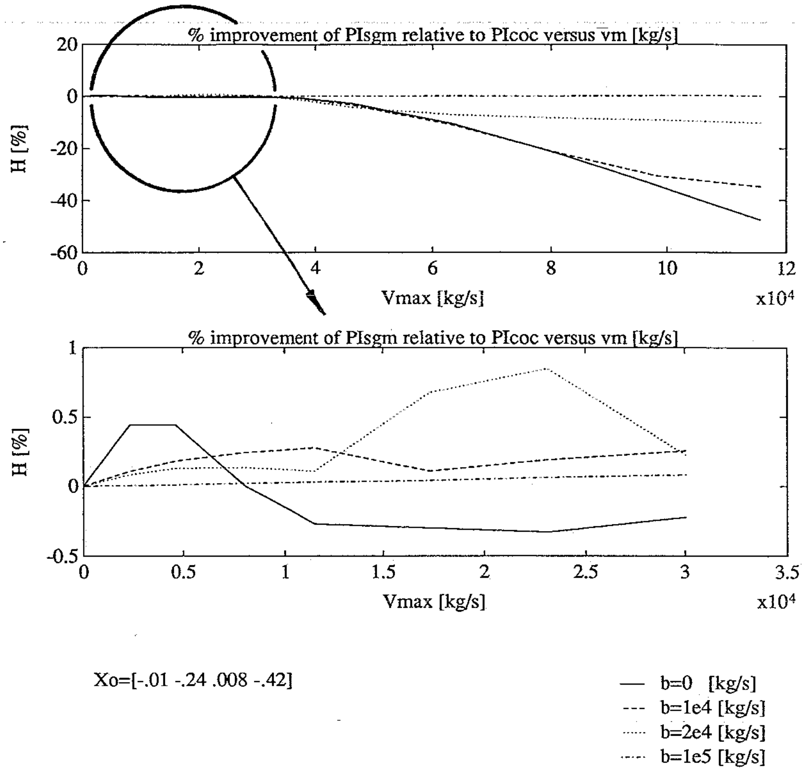

Figure 5.1: The effect of Saturation Bounds

weighting factors.

The Effect of Weighting Factors:

Figure 5.2 shows the proportional improvement of SGC relative to COC (H) versus q_1, for different values of q_2. Where q_1 and q_2 are the weighting factors of respectively the suspension- and the tire deflection.

The conclusion is that the effect of weighting factors on the proportional improvement is substantial, but because of the nonlinear system no prediction can be made how the weighting factors affects H.

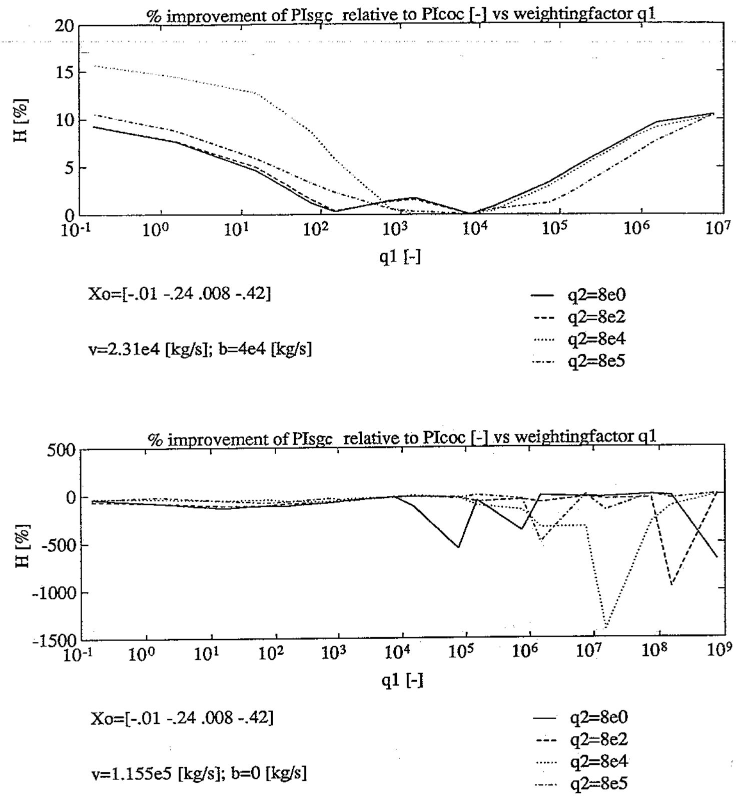

Figure 5.2: The effect of Weighting Factors

5.3 Simulations with rounded pulse excitation

The second excitation is the excitation by rounded pulses. Rounded pulses or bumps can be discribed by two parameters t_d and $z_{r\ max}$, where t_d represents the time needed to pass 96% of the bump and $z_{r\ max}$ is the maximum amplitude of the pulse. These parameters are chosen such that the response of the passive system[1] does hit the bounds of either the tire deflection or the suspension deflection. Fig. 5.3 shows the general form of the rounded pulses.

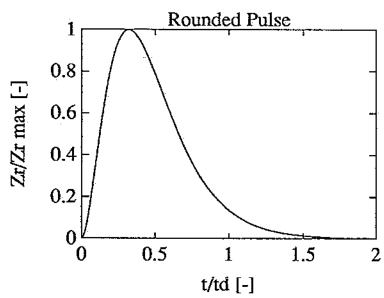

Figure 5.3: Rounded Pulse

Simulations have been executed on 20 different road bumps. The values of t_d and $z_{r\ max}$

[1] $v = 0$ [Ns/m]; $b = 43,1$ [kNs/m]

of each bump are shown in tabel 5.3.

t_d [s]	$z_{r\ max}$ [m]	t_d [s]	$z_{r\ max}$ [m]
1.00E-2	5.20E-2	3.06E-1	1.02E-1
2.20E-2	2.64E-2	3.44E-1	1.09E-1
4.84E-2	1.87E-2	3.87E-1	1.17E-1
7.14E-2	1.93E-2	4.36E-1	1.26E-1
1.06E-1	2.36E-2	5.10E-1	1.40E-1
1.29E-1	2.82E-2	7.56E-1	1.76E-1
1.59E-1	3.56E-2	1.12E0	2.29E-1
1.91E-1	4.82E-2	2.46E0	4.85E-1
2.32E-1	7.08E-2	5.40E0	1.34E0
2.72E-1	9.60E-2	1.18E1	4.65E0

Tabel 5.3: Parameters of the rounded pulses

In figure 5.4 the maximum and minimum suspension- and tire deflection and the maximum absolute value of the body acceleration are plotted versus t_d for the Clipped Optimal and the Steepest Gradient control law. These quantities are used to judge the reponse of the system to the different roadbumps.

To investigate the differences between COC and SGC, we consider the proportional differences between SGC and COC for the defined criteria. In figure 5.5 these quantities are plotted versus t_d.

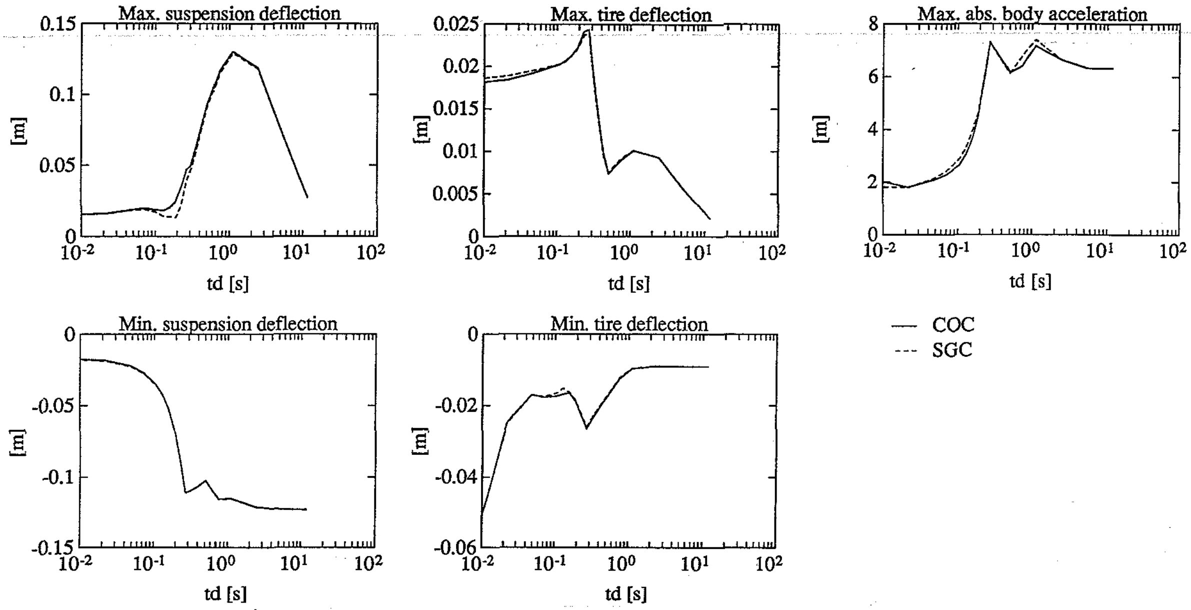

Figure 5.4: Response on 20 rounded pulses

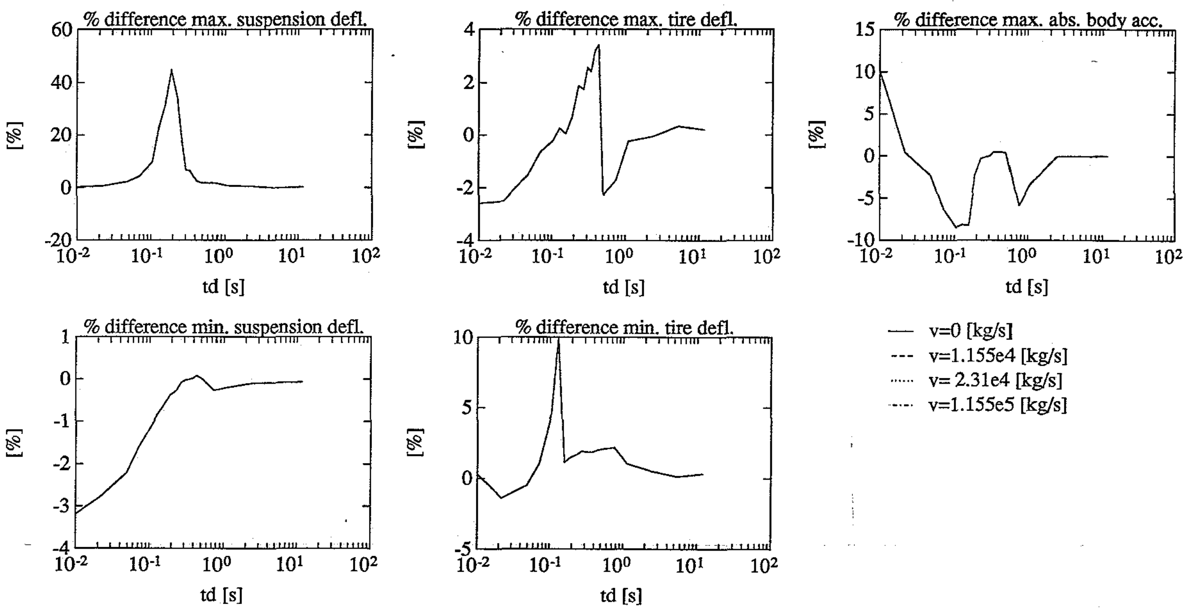

Figure 5.5: Proportional Difference between SGC and COC

From this figure we perceive that both SGC and COC perform differently for different road bumps. At the same time different performance can be recognized for different criteria. The performance and the difference in performance between COC and SGC strongly depends on the used saturation bounds and the used weighting factors. No relation can be found for the distinction in performance between SGC and COC.

The Effect of Saturation Bounds:

To inquire the effect of saturation bounds the above mentioned proportional difference between SGC and COC is plotted versus t_d for different values of v_{max} in fig. 5.6.

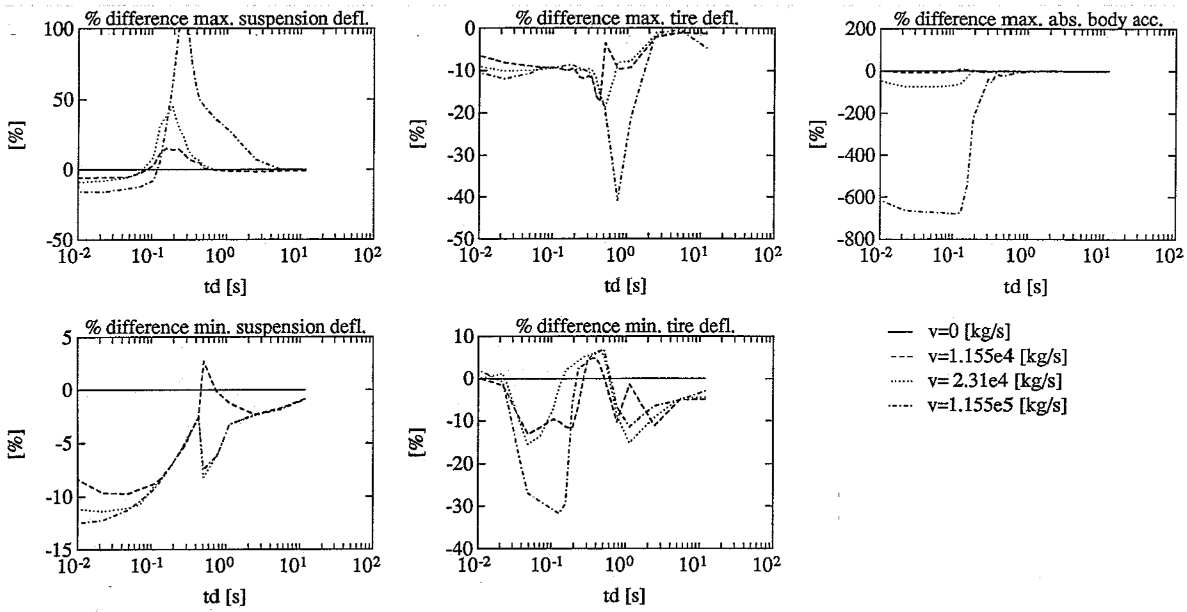

Figure 5.6: Effect of Saturation Bounds when $b = 0$ [Ns/m]

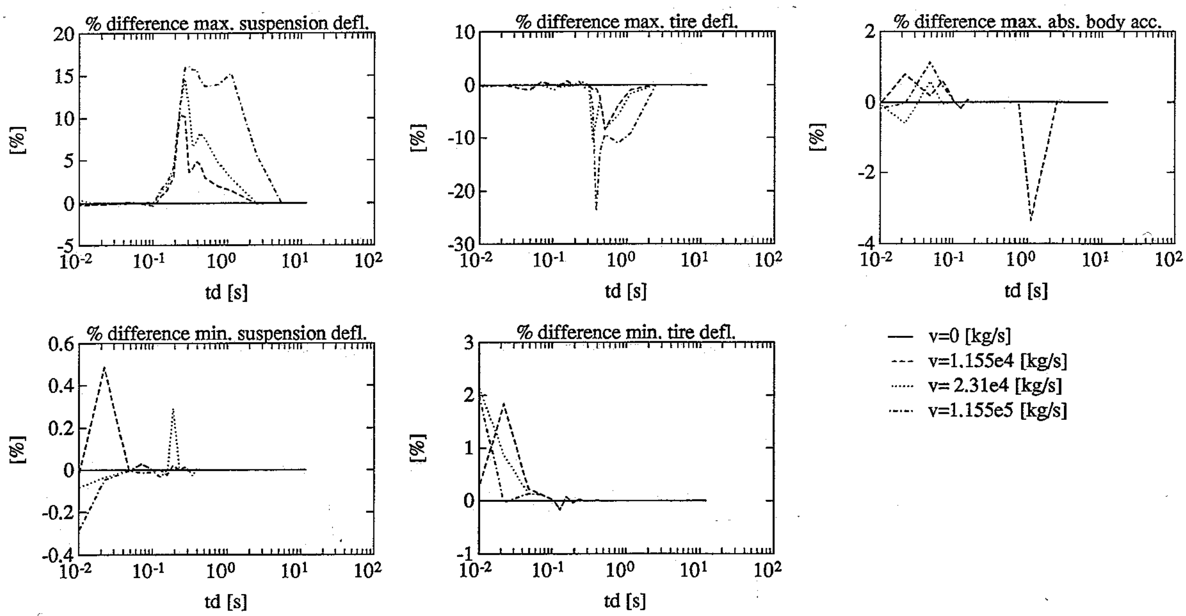

Figure 5.7: Effect of Saturation Bounds when $b = 40$ [kNs/m]

The conclusion from this figure is: the higher v_{max} the higher the differences in performance between SGC and COC for the maximum suspension- and tire deflection. At the same time the maximum absolute value of the body acceleration of COC is shown to become smaller than that of the SGC when the saturation bound increases.
When the same figure is plotted in the case of $b = 40$ [kNs/m], figure 5.7 arises.

By taking fig. 5.6 and fig. 5.7 into account we can conclude that when b increases the difference between SGC and COC decreases for all criteria.

The Effect of Weighting Factors:

Many simulations have been executed for different weighting factors. The conclusion from these simulations is that the weighting factors affect the performance substantially, but due to the nonlinearity of the system no relation can be found.

5.4 Simulations with a stochastic road excitation

In reality the suspension of a vehicle is not excited by initial condition disturbances or single rounded pulses but by road surfaces that consist of a combination of long and short irregularities. For this reason simulations have been executed on a stochastic road which contains all relevant frequenties.

A realization of this stochastic road surface is generated by summing 1000 sinusoidals with randomly distributed frequenty between $f_{min} = 0.1$ [Hz] and $f_{max} = 50$ [Hz]. The sine waves have a uniformly distributed random phase and an amplitude that is determined by the following Power Spectral Density (PSD):

$$
\begin{aligned}
PSD &= \begin{cases} R_c \frac{v^{\kappa-1}}{f_0{}^{\kappa}} & \text{if } f < f_0 \\ R_c \frac{v^{\kappa-1}}{f^{\kappa}} & \text{if } f > f_0 \end{cases} \\
f_0 &= \lambda v
\end{aligned}
\tag{5.3}
$$

Where R_c a measure of the roughness of the road, κ the slope of the density function, v the driving speed and λ the cycle number. For these parameters the following values have been used:

$$
\begin{aligned}
R_c &= 5.297\text{e-}6 && [m^2(m/cycle)^{p+1}] \\
\kappa &= 1.974 && [\text{-}] \\
v &= 13.9 && [\text{m/s}] \\
\lambda &= 0.01 && [\text{cycle/m}]
\end{aligned}
$$

The power spectral density function and a realization of the stochastic road surface are plotted in figure 5.8 respectively in figure 5.9.

The criteria to judge the resonse of the system are the Root-Mean-Square values of the suspension deflection, the tire deflection and the sprung mass acceleration.

The Effect of Saturation Bounds:

To inquire the effect of saturation bounds three simulations have been excited for different constant and variable damping coefficients. Tabel 5.4 shows the results.

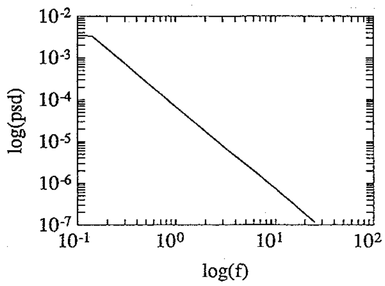

Figure 5.8: PSD function of the stochastic road surface

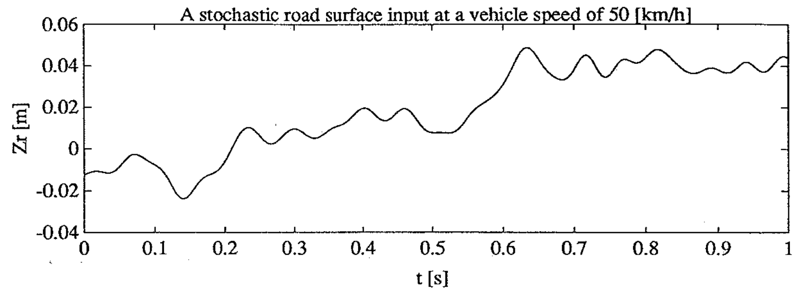

Figure 5.9: A realization of the stochastic road surface

b $\left[\frac{kNs}{m}\right]$	v_{max} $\left[\frac{kNs}{m}\right]$	Root-Mean-Square value					
		Suspension deflection $[mm]$		Tire deflection $[mm]$		Body acceleration $\left[\frac{m}{s^2}\right]$	
		COC	SGC	COC	SGC	COC	SGC
20	23.1	14.4	13.1	6.3	6.1	1.34	1.37
20	115.5	15.2	25.5	8.2	8.9	1.02	2.25
100	115.5	8.10	8.20	4.5	4.5	2.50	2.50

Tabel 5.4: The effect of Saturation Bounds

From tabel 5.4 the following conclusions can be drawn. When v_{max} increases COC performs substantially better than SGC. And when b increases, the improvement of COC decreases. These conclusions harmonize with the conclusions from the other two excitation forms.
Because of the calculation time no simulations have been executed for different weighting factors.

Chapter 6

Conclusions

The conclusion can be drawn that the performance of the Clipped Optimal and the Steepest Gradient control law strongly depend on the used set of parameters. Simultaions have been executed for different weighting factors and for different saturation bounds.
The effect of the weighting factors is substantial but an obvious formula which describes the influence can not be found.
It is shown for all excitation forms that the effect of saturation bounds on the performance of Clipped Optimal is more or less equal to that of Steepest Gradient when the control saturation is significant or when the constant dampingcoefficient is large. When the saturation bound is large and and the constant dampingcoefficient is small Clipped Optimal performs substantial better than Steepest Gradient.

Bibliography

[1] H.E. Tseng, K. Yi, and K.J. Hedrick,
A comparison of Alternative Semi-active Control Laws,
Advanced Automotive Technologies, DE-Vol. 40, 1991 ASME

[2] Butsuen T. and Hedrick J.K. 1989,
Optimal Semi-active Suspensions for Automotive Vehicles: The $\frac{1}{4}$ car model,
Advanced Automotive Technologies -1989, Dsc-Vol. 13, 1989 ASME WAM.